Aerodynamics during forward flight of a tailless flapping-wing micro air vehicle

L.T.K. Au and H.C. Park*

Konkuk University, Department of Smart Vehicle Engineering

ABSTRACT

In this paper, the aerodynamic performance during forward flight of KU-Beetle—an insect-like flapping-wing micro air vehicle (FW-MAV) is studied. A range of advance ratio (J) from 0 to 0.5 was considered. The aerodynamic forces and pitching moment could be manipulated by adjusting two parameters: the wing-root angle (γ) and stroke plane angle (β). For each investigated advance ratio, the aerodynamic forces and pitching moment for a pair of β and γ was computed by computational fluid dynamics (CFD) method via commercial software of ANSYS Fluent 16.2. The average values taken at third flapping cycle when the flow was settled could be obtained. The equilibrium for an advance ratio, in which the drag and pitching moment on the body were balanced by horizontal force and pitching moment produced by the wing respectively, was acquired using Newton-Raphson method. The study shows that for flapping angle (ψ) in range from -90° to 90°, the inflow due to forward flight augmented the total inflow velocity during downstroke, and reduced the total inflow during upstroke. This results in "reverse region"—a part of the wing starting from wing root where the total inflow direction during upstroke was reversed. In this reverse region, the lift was negative, which reduced the lift produced by the whole wings. The region enlarged when the forward flight speed increased. Therefore, compared to hovering, for the same stroke plane angle, during forward flight, the wings produced more drag during upstroke and less thrust during downstroke, resulting in larger drag; meanwhile, the wings produced more lift during upstroke and less lift during downstroke, hence the change of

lift is insignificant. To balance drag during forward flight, KU-Beetle must incline forward, so that the horizontal component of the lift can overcome the drag. When J=0.5, the body inclined 40° which is a little larger than that of a bumble bee.

1 INTRODUCTION

Insects' extraordinary flight ability has drawn attention of scientists for over a century. It has been proven that the conventional aerodynamics model based on translational force cannot estimate sufficient lift for hovering insects [1]. Therefore, numerous efforts have been carried out to reveal the underlying force augmentation mechanisms of flapping flight, and considerable progress in aerodynamics of insect flight has been achieved in recent decades. These include clap-and-fling, leading edge vortex created by delayed stall, rotational circulation and wake capture functioning during stroke reversal and added mass. The influences of wing-wake interaction, wing-wing interaction on the production of aerodynamic forces in four-winged insects were also widely studied. With these discoveries, quasi-steady aerodynamic model was modified to improve the accuracy in estimation of aerodynamic force produced by flapping wings [2].

Among the flight regimes of insect flight, hovering received the most attention from scientists. This flight regime is the first goal in most flapping-wing micro air vehicle development. There are also considerable studies in forward flight, in both areas of aerodynamics and dynamic flight stability. Recently, Han et al. proposed a semi-empirical quasi-steady aerodynamic model for

force estimation during forward flight of flapping flyers [3]. Although forward flight in insects has been extensively studied, the aerodynamics during forward flight of a flapping-wing micro air vehicle (FW-MAV) remains limited in literature survey. In this paper, we report the aerodynamic performance in forward flight of KU-Beetle, a tailless FW-MAV. A range of advance ratios (J), which is the ratio between the forward flight speed and the mean tip speed, from 0 to 0.5 was investigated.

2 MATERIAL AND METHOD

Section headings should be numbered, centre justified and in all capitals. Font size shall be 11pt. Sub-headings are left justified, numbered and italic.

2.1 Wing kinematics

In KU-Beetle, the aerodynamic forces and pitching moment can be manipulated by changing the angle γ between the wing root and the body line, as shown in Fig. 1 (Phan et al. 2016 [4]). When γ is changed, the wing deformation is adjusted, resulting in control forces and pitching moment.

The motion of the left wing is described in Figure 2a. The wing simultaneously flaps around the flapping axis (z-axis) and pitches around the feather axis (ξ-axis). The feather axis is attached to the leading edge of the wing. The location of the feather axis is determined by the flapping angle ψ. Each wing section was treated as a parabolic curve whose shape could be determined by two parameters. The first one is the mid-chord rotation angle ϑ_m—the angle between the stroke plane and the line connecting the leading edge to the mid-chord position. The second one is the full-chord rotation angle ϑ_r—the angle between the stroke plane and the line connecting the leading edge to the trailing edge. The variations of ψ, ϑ_m and ϑ_r versus time were captured by hi-speed cameras. These data were fitted by sums of sinusoidal functions.
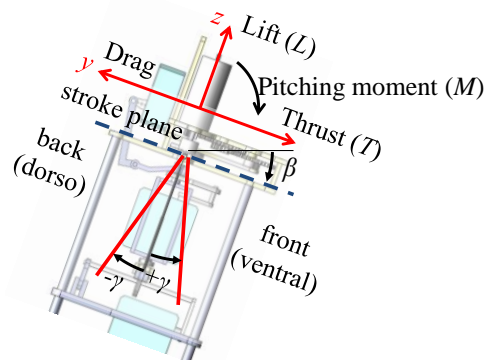

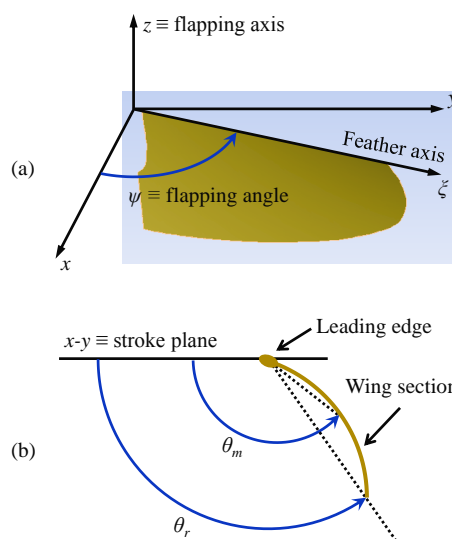**Figure 1 - Control variable, the red lines indicate the wing root**

Figure 2 - Wing motion. (a) Three-dimensional wing motion. (b) Wing camber

2.2 Computational fluid dynamics model

The forces and pitching moments acting on the wing and the body frame were computed separately using CFD method. Figure 3 illustrates the computational domain and wing geometry. The wing was modeled as a membrane twisted from the root to tip. Because of longitudinal symmetrical plane, the CFD model was built for only left wing. Therefore, the computational domain is a half cylinder. The size of the computational domain was chosen such that the diameter and the length are twelve times the distance from the wing root to tip (wing length).

The mesh is finest around the wing, and become coarser toward the far-filed region, as shown in

Fig. 4. A high density region whose diameter doubles the wing length was built around the wing. The wing surface was meshed by approximately 21,000 triangle elements.
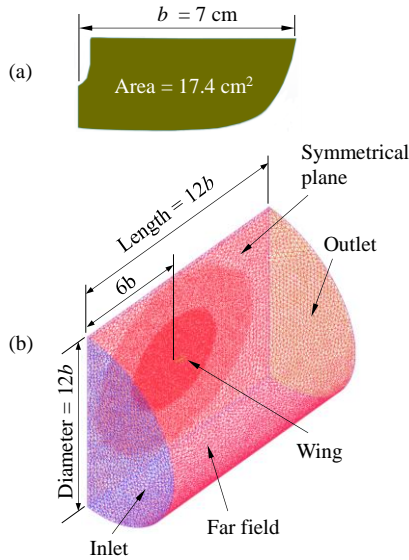

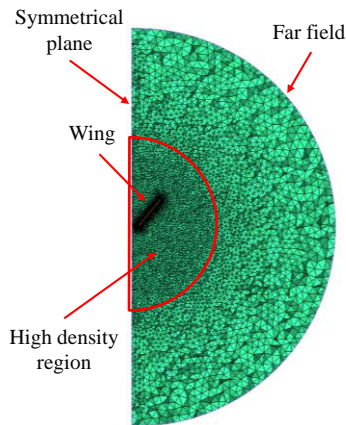Figure 3 - (a) Wing geometry. (b) Computational domain

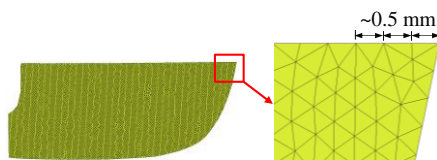Figure 4 - A cross section of the volume mesh

Figure 5 - Mesh on the wing surface

3 RESULT AND DISCUSSION

3.1 Effect of forward flight on force generation

The total inflow velocity is expressed as follows:

$$\vec{V}_{inflow} = V_{inflow}\vec{e}_T = V_T\vec{e}_T + U\vec{e}_T, \qquad (1)$$

where V_T and U are the inflows due to flapping motion and due to forward flight, respectively, and $\vec{e}_t$ is the unit vector points in direction of inflow due to translational motion. These quantities can be expressed as follows:

$$V_T = \begin{cases} -r\dot{\psi} & \text{during downstroke} \\ r\dot{\psi} & \text{during upstroke} \end{cases}$$

$$U = \begin{cases} V_f\cos\psi & \text{during downstroke} \\ -V_f\cos\psi & \text{during upstroke} \end{cases} \qquad (1)$$

Therefore, V_{inflow} can be expressed as follows:

$$V_{inflow} = \begin{cases} -r\dot{\psi} + V_f\cos\psi & \text{during downstroke} \\ r\dot{\psi} - V_f\cos\psi & \text{during upstroke} \end{cases} \qquad (2)$$

A negative V_{inflow} means that the inflow is reversed, and the translation lift produced by the wing is negative. The total inflow during downstroke and upstroke are illustrated in Fig. 6. For -90<ψ<90°, $V_f\cos\psi$>0, hence, the inflow due to forward flight augments the total inflow velocity during downstroke, and reduces the velocity during upstroke, as shown in Fig. 6a,b. On the other hand, when ψ<-90° or ψ>90°, $V_f\cos\psi$>0, hence, the inflow due to forward flight reduces the total inflow velocity during downstroke, and augments the velocity during upstroke, as shown in Fig. 6c,d. As a result, for -90<ψ<90°, the reverse region appears during upstroke, while for ψ<-90° or ψ>90°, the region appears during downstroke. The flapping angle of current FW-MAV is from -93° to 90°. That means the portion when ψ<-90° or ψ>90° is negligible compared to that when -90<ψ<90°. As a result, in most of the flapping cycle, the reversed flow appears during upstroke, which explains the reduction in lift and thrust during upstroke, and augmentation in lift and drag during downstroke, as plotted in Fig. 7.
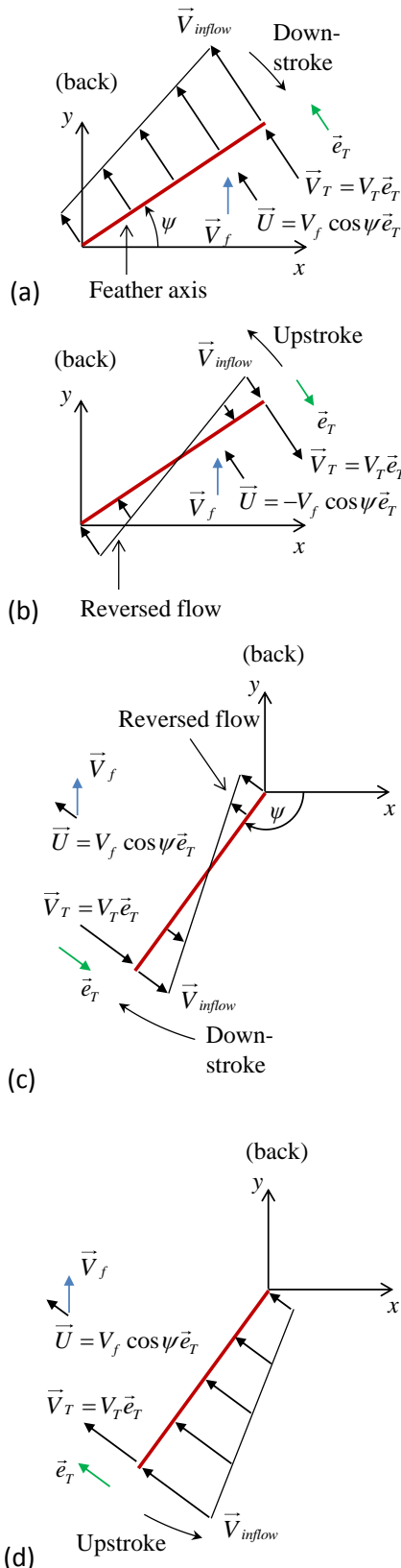
(a)

(b)

(c)

(d)

Figure 6 - Inflow in KU-Beetle. (a) During downstroke, −90<ψ<90°. (b) During upstroke, −90<ψ<90°. (c) During downstroke, ψ<−90° or ψ>90°. (d) During upstroke, ψ<−90° or ψ>90°.

The mean lifts and drags for various advance ratios J ranging from 0 to 0.5 are listed in table 1. As J increases, the mean lift and drag increase during downstroke, while the lift and thrust decreases during upstroke. As a result, the total mean lift over one flapping cycle does not change much. while the total mean drag increases when J enlarges.

	Stroke	$J=0$	$J=0.25$	$J=0.5$
Lift [gf]	Down	9.23	16.63	23.22
	Up	10.46	7.00	5.90
Drag [gf]	Stroke	J=0	J=0.25	J=0.5
	Down	5.20	10.93	16.97
	Up	-5.56	-2.88	-2.42

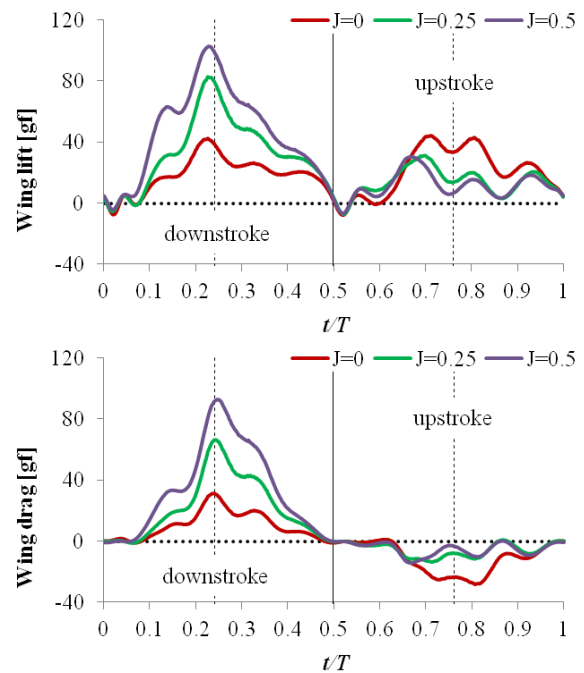**Table 1 - Mean lift and drag for various Js**

Figure 7 - Time-course lift and drag for various Js

3.2 Equilibrium forward flight

For each advance ratio J, the equilibrium flight condition can be achieved by adjusting the wing root angle γ and the stroke plane angle β. The pair (γ, β) can be found using Newton-Raphson method. Let H be the force in backward horizontal direction, and M be the

pitching moment. At equilibrium, the total H and M of the body and the wings equal to 0. The flow chart using Newton-Raphson algorithm for acquiring the pair (γ_e, β_e)–values of γ and β when the equilibrium for an advance ratio J is achieved–is illustrated in Fig. 8.
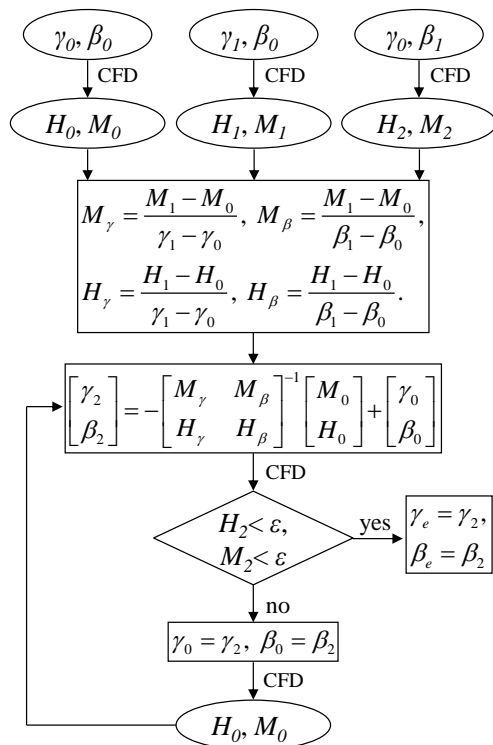

Figure 8 - Flow chart for acquiring equilibrium

The equilibrium stroke plane angle for various J is plotted in Fig. 9. The result of bumble bee is plotted in the same figure for comparison. For forward flight, KU-Beetle must incline forward, so that the horizontal component of the lift can overcome the increasing drag on the wing and the body frame. This result has similar trend to that of bumble bee.
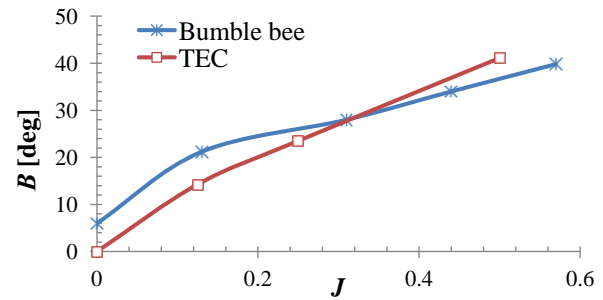

Figure 9 - Stroke plane angle for equilibrium during forward flight

4 CONCLUSION

The aerodynamics during forward flight of KU-Beetle—a tailless FW-MAV was investigated using CFD method. Because of the inflow due to forward flight, the inflow increases during downstroke, and decreases during upstroke. This results in augmentation in lift and drag during downstroke, and reduction in lift and thrust during upstroke. The equilibrium flight condition was acquired using Newton-Raphson method. To achieve equilibrium as the forward flight speed increases, KU-Beetle must incline forward, which means that the stroke plane angle increases.

ACKNOWLEDGEMENTS

REFERENCES

[1] Ellington C P. The aerodynamics of hovering insect flight. I. I. The quasi-steady analysis. *Philosophical Transactions of the Royal Society of London B*, 1984, **305**, 1-15

[2] Truong Q T, Nguyen Q V, Truong V T, Park H C, Byun D, Goo N S. A modified blade element theory for estimation of forces generated by a beetle-mimicking flapping wing system. *Bioinspiration & Biomimetics*, 2011, **6**, 1-11.

[3] Han J S, Chang J W, Han J H. An aerodynamic model for insect flapping wings in forward

flight. *Bioinspiration & Biomimetics*,2017, **12**, 1-16.

[4] H. P. Phan, T. Kang and H. C. Park, "Design and stable flight of a 21 g insect-like tailless flapping wing micro air vehicle with angular rates feedback control," *Bioinspiration & Biomimetics*, volume 12, 2017, 17pp. Dynamic flight stability of a hovering bumblebee. *Journal of Experimental Biology*, 2005, **208**, 447-459.